Electronic structure and Fermi surface of paramagnetic and antiferromagnetic UPt_2Si_2

S. Elgazzar,[1,*] J. Rusz,[2] P. M. Oppeneer,[2] and J. A. Mydosh[3]
[1]*Department of Physics, University of Johannesburg, P.O. Box 524, Auckland Park 2006, South Africa*
[2]*Department of Physics and Astronomy, Uppsala University, Box 516, S-75120 Uppsala, Sweden*
[3]*Kamerlingh Onnes Laboratory, Leiden University, NL–2300 RA Leiden, The Netherlands*
(Received 13 June 2012; published 6 August 2012)

We report density functional theory-based calculations of the electronic structure and Fermi surface properties of the intermetallic uranium compound UPt_2Si_2, which orders antiferromagnetically at $T_N = 32$ K with a total magnetic moment of $2\mu_B$/U-atom and exhibits a moderate mass enhancement in the specific-heat coefficient. Our investigation is carried out using relativistic, full-potential band-structure methods within the framework of the local spin density approximation (LSDA), the LSDA with orbital polarization correction (LSDA + OPC), and the LSDA supplemented with an additional Hubbard U (LSDA + U). We find that the LSDA + OPC scheme predicts the total magnetic moment in best agreement with experiment; from this we infer that the $5f$ electrons in UPt_2Si_2 are orbitally polarized, mostly itinerant, and exhibit only a slight tendency toward localization. Our total energy calculations predict UPt_2Si_2 to form in the $CaBe_2Si_2$ ($P4/nmm$) structure, in contrast to URu_2Si_2 ($ThCr_2Si_2$: $I4/mmm$). The theoretical Fermi surfaces are also studied for the nonmagnetic and antiferromagnetic phases with the employed computational schemes and are found to be quasi-two-dimensional. At the antiferromagnetic transition, the Fermi surface is found to become more two-dimensional with small regions of gapping.

DOI: 10.1103/PhysRevB.86.075104 PACS number(s): 78.20.−e, 71.20.−b, 71.28.+d

I. INTRODUCTION

The uranium-based intermetallic compound UPt_2Si_2 has been studied for many years,[1–3] yet a complete understanding of its electronic properties remains absent. This material represents an archetypal U-compound[4] in which the $5f$ electrons do not strongly hybridize with the conduction electrons and thereby moderate-size magnetic moments remain in the ground state. Such behavior is in stark contrast to the heavy Fermi liquid formation of the polymorph 122 compound URu_2Si_2, where a nonmagnetic "hidden-order" transition[5] allows for an unconventional superconducting ground state.[6] Conversely, for UPt_2Si_2 with its small mass enhancement, one may expect an antiferromagnetic ground state with somewhat reduced U-moments ($\approx 2.0\mu_B$) below $T_N = 32$ K, and this has been firmly established to occur with a simple alternation of ferromagnetic planes along the longer c axis.[3] The reason for the dissimilar behavior between URu_2Si_2 and UPt_2Si_2 is thought to lie in the different crystal structures: $ThCr_2Si_2$ ($I4/mmm$) versus $CaBe_2Si_2$ ($P4/nmm$), respectively. The latter seems to support subtle forms of disorder, thereby preventing the formation of a coherent Fermi liquid. For UPt_2Si_2, the concept of *strain disorder* has been employed based upon the observed large thermal displacement factors causing random nearby vacancies for certain Pt and Si sites.[7,8] It remains an open question why this subtle disorder plays so dramatic a role in the formation of the U-ground state and so greatly affects the transport properties over a wide temperature range.[7] Only for a few U intermetallic compounds, e.g., URh_2Ge_2, UCu_4Pd, and UAsSe, has the nature of the disorder been investigated and determined.[7,9–11]

By comparing various U-based 122 compounds[12] of both the $I4/mmm$ and $P4/nmm$ crystal structures, we note a similarity in their transport properties. At high temperature (100–300 K), the longer c axis exhibits a large negative-temperature coefficient resistivity exceeding the Mooij limit of $\sim 250\ \mu\Omega$ cm. In contrast, the in-plane a axis shows a much smaller resistivity characteristic of a good metal. We attribute this seemingly generic behavior of these U compounds to their semimetallic state with a partial gapping and reduced carrier concentration along the c direction. When coupled with the crystal disorder tendency of the $P4/nmm$ structure, we have an additional scattering mechanism (disorder-induced localization) over and above that of spin fluctuations and spin disorder of the U moments. Resistivity, Hall effect, and optical conductivity experiments have revealed a glassylike electronic transport,[13] attributed to strong electronic correlations coupled to the disorder. At lower temperature, there is the antiferromagnetic order or the formation of the heavy Fermi liquid states. So here the resistivity can decrease to its structural disorder limit, if any. It is these large scattering mechanisms in conjunction with the low carrier density of the anisotropic semimetal that govern the resistivity behavior. Such effects should also be reflected in the other magnetoelectronic transport properties. Very recently, studies of the antiferromagnetic phase in UPt_2Si_2 have been performed in high magnetic fields up to 40 T.[14,15] Such measurements have uncovered a series of field-induced phase transitions.

While URu_2Si_2 has been the focus of many electronic structure calculations,[16–18] UPt_2Si_2 has been completely neglected. Due to their different crystal structures and lattice constants, significant alterations are expected in the band structure of UPt_2Si_2. Therefore, the results of our density functional theory (DFT) study should aid in fully describing the experimental properties and confirming the above experimental conclusions.

Recently, the thermal magnetic transport properties of UPt_2Si_2 have been examined[19] and large anomalies were found near T_N in the Nernst (e_N) and Seebeck (S) effects, thermal conductivity (κ), the Hall (R_H) effect, and electrical resistivity (ρ). Such anomalies identify a weak superzone or pseudogap which appears below the onset of antiferromagnetism. While ρ and $d\rho/dT$ display a tiny indication of superzone gapping for current along the c axis, none is visible within the ($a \times a$)

ferromagnetic planes. The opposite is true for e_N; only ΔT parallel to the a axis with a magnetic field along c produces a clear Nernst signal. These anomalies have been described by theoretical model calculations[20,21] using a free-electron relaxation time model. Here the antiferromagnet is anticipated to possess a superzone gap due to the inequivalence of the two U sites occurring in the simple tetragonal ($P4/nmm$) structure. This charge gap when combined with spin and phonon scattering causes a large contribution to e_N and S while the ρ shows a much smaller effect. There is overall good experimental and theoretical agreement for UPt_2Si_2 regarding the measured and calculated temperature dependences, and also a scaling law predicted by theory between e_N and $(S \times R_H)$ has been nicely verified for UPt_2Si_2 but not for URu_2Si_2.[19] Since we expect that a partial charge gap should appear in the antiferromagnetic state, it is meaningful to attempt to locate the gapping effects on the Fermi surface (FS) and in the density of states (DOS) by comparing the paramagnetic and antiferromagnetic FS. This requires state-of-the-art electronic structure calculations for UPt_2Si_2 which presently have not yet been performed.

In this work, we present the results of such DFT-based calculations via the local density approximation (LDA) for the paramagnetic state and the local spin density approximation (LSDA), the LSDA with orbital polarization correction (LSDA + OPC), and the LSDA supplemented with an additional Hubbard U (LSDA + U) for the antiferromagnetic state. We find a twofold change in the DOS at the Fermi level (E_F) when crossing the magnetic transition. Furthermore, we can locate the FS modifications to certain regions in the Brillouin zone. We then compare these results with the known experimental properties. It is especially interesting to relate the experimental anisotropy to the regions of FS gapping and to resolve the dichotomy between resistivity and Nernst behavior, thereby allowing the thermal magnetic properties to be used as a tool in determining the anisotropic gapping effects of a generic antiferromagnet.

II. COMPUTATIONAL METHODS

The electronic structure calculations were carried out employing two relativistic full-potential band-structure methods, namely the full-potential local orbital (FPLO) minimum-basis band-structure method[22] and the full-potential linearized augmented plane waves method in the WIEN2K implementation.[23]

In the relativistic FPLO version,[24,25] the four-component Kohn-Sham-Dirac equation, which contains spin-orbit coupling up to all orders, is solved self-consistently. In these calculations, the following basis sets were adopted for the valence states: the $5f; 6s6p6d; 7s7p$ states for U (note that the uranium $5f$'s are treated as valence states), and for Pt and Si we used $5s5p5d; 6s6p$ and $3s3p3d$, respectively. The high-lying $7s$ and $7p$ semicore states of U, which might hybridize with the $6d$ and $5f$ valence states, are thus included in the basis. The site-centered potentials and densities were expanded in spherical harmonic contributions up to $l_{\max} = 12$. The number of **k** points in the irreducible part of the Brillouin zone (BZ) was 196, but calculations were made also with 405 and up to 2176 **k** points to resolve the density of states at the Fermi energy (E_F). The Perdew-Wang[26] parametrization of the exchange-correlation potential in the LSDA was used. Due to the underlying homogeneous electron gas assumption, the standard LDA and LSDA exchange-correlation functionals provide suitable results when the $5f$ electrons are fully itinerant. However as mentioned above, this assumption cannot be straightforwardly made for UPt_2Si_2. We therefore use two further schemes to probe the behavior of the uranium $5f$ states, viz., the orbital polarization correction and the LSDA + U. The orbital polarization correction was introduced by Brooks[27]; we employ here the recent OPC formulation of Ref. 28. The OPC is expected to provide an improved description of magnetic materials with more localized magnetic moments where there exists a dominant orbital magnetization.

The nonmagnetic and antiferromagnetic FPLO calculations were compared to results obtained with the WIEN2K code[23] (which includes spin-orbit coupling[29] and local orbitals) and a good agreement was found. The WIEN2K code was also used for LSDA + U calculations of an antiferromagnetic phase of UPt_2Si_2, which are reported below. The around mean field (AMF) variant of the LDA + U potential was used.[30] The value of U was set to 2.0 eV and the value of J to 0.5 eV. In these calculations, we used atomic sphere radii of 2.8, 2.4, and 2.0 atomic units for U, Pt, and Si, respectively. The $RK_{\max}$ parameter, which determines the basis size, was set to 7.5 leading to approximately 120 basis functions per atom. For the BZ integrations, we have used 390 **k** points inside the irreducible wedge, which corresponds to approximately 5000 **k** points in the whole first BZ.

At this point, we note that although the employed DFT-based band-structure methods allow us to capture varying degrees of U $5f$ localization, from delocalized (with LSDA) to moderately localized (with LSDA + U), the influence of the crystallographic disorder[7,8] on the degree of $5f$ localization cannot be so easily addressed.

III. RESULTS AND DISCUSSIONS

A. Volume optimization

The compound UPt_2Si_2 crystallizes in the simple tetragonal $CaBe_2Si_2$ ($P4/nmm$) structure with space group No. 129 for the nonmagnetic (PM) and (hypothetical) ferromagnetic (FM) phases. In our band-structure calculations, we used the recently published experimental lattice parameters: $a =$ 4.186 Å and $c = 9.630$ Å and the atomic positions as U (0.25, 0.25, 0.7484), Pt (0.25, 0.25, 0.3785), Pt (0.75, 0.25, 0), Si (0.75, 0.25, 0.5), and Si (0.25, 0.25, 0.133).[7] When the compound orders antiferromagnetically, the two uranium sublattices become inequivalent and the structure becomes simple tetragonal with space group No. 99. This space group and the above-mentioned lattice parameters[7] have been used for calculations of antiferromagnetic (AFM) UPt_2Si_2. Figure 1 exhibits the crystal structure along with the Brillouin zones and the irreducible wedges corresponding to the two space groups.[31] The irreducible wedge doubles for the AFM phase, and the mirror symmetry in the $k_z = 0$ plane of the PM phase is broken.

We have calculated the total energy for the $P4/nmm$ structure compared to the fictional $I4/mmm$ structure of UPt_2Si_2. The minimum energy clearly resides with the

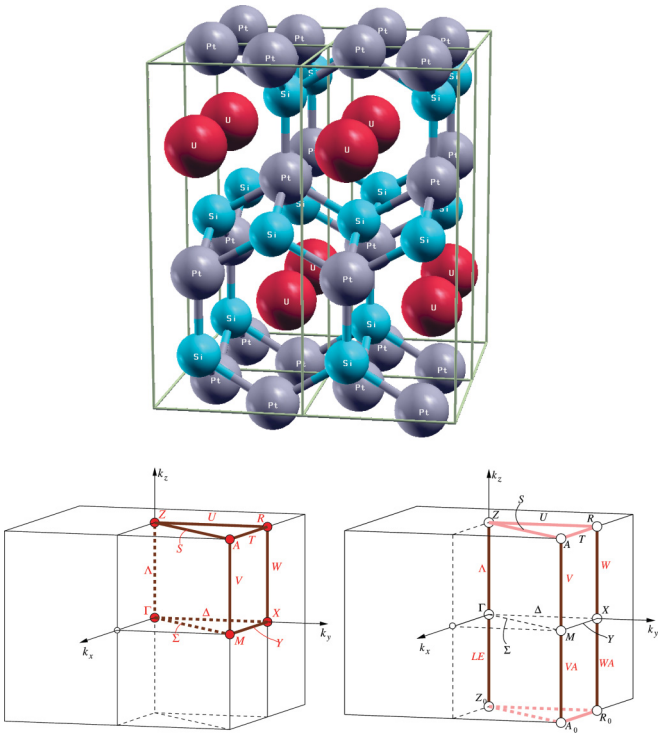

FIG. 1. (Color online) The crystal structure of antiferromagnetic UPt_2Si_2 (simple tetragonal, space group No. 99). Four unit cells are shown, doubling the primitive unit cell along a and b axes, to highlight the uranium layers and cages of silicon and platinum around them. In the nonmagnetic state, the two uranium sublattices become equivalent and the structure is simple tetragonal with space group No. 129. The lower-left panel shows the simple tetragonal Brillouin zone with an irreducible wedge for space group 129 and the lower-right panel shows that of space group 99 (from Ref. 31).

$P4/nmm$ space group, being favored by 24.573 meV per formula unit (f.u.). This confirms its different crystal structure when compared to URu_2Si_2; we also note that Pt has two additional $5d$ electrons relative to $4d$ Ru. Thus, UPt_2Si_2 is distinctly different from URu_2Si_2. A further calculation has been performed for the total energy versus volume for the three possible magnetic phases: PM, FM (space group No. 129), and AFM (No. 99). The calculated results are displayed in Fig. 2. We observe that AFM has a lower total energy than FM and PM in agreement with experiment, and that the LSDA minimum volume is slightly lower (by 0.14%) than the experimental volume, a common trend with LSDA calculations. Furthermore, we have calculated the equation of state, the bulk modulus B_0, and its pressure derivative, B_0'. The computed volume versus pressure is shown in the inset of Fig. 2. The calculated values for the AFM ground state are $B_0 = 196.6$ GPa and $B_0' = 4.0$. At present, there are no measured compressibility data available. We note, however, that high-pressure x-ray diffraction measurements on UPt_2Si_2 have shown the absence of a pressure-induced crystallographic phase transition up to 25 GPa.[33]

B. Energy dispersions

A detailed picture of the electronic structure near the Fermi level can be obtained from a band-structure plot for PM and

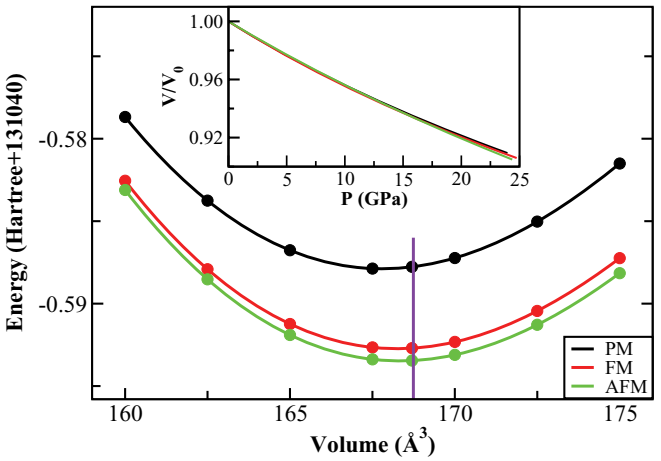

FIG. 2. (Color online) The calculated L(S)DA total energy as a function of volume for UPt_2Si_2 in PM, FM, and AFM phases, respectively; see text. The vertical line denotes the experimental volume.[7] Inset: Normalized unit-cell volume, $V(P)/V_0$, as a function of pressure for UPt_2Si_2 calculated by the Birch-Murnaghan equation of state.[32]

AFM UPt_2Si_2. In Fig. 3 (top), we show the LDA energy band dispersions of nonmagnetic UPt_2Si_2 in the vicinity of E_F using the experimental lattice constants and space group (No. 129). Here we find four bands which cross the Fermi energy. These bands are denoted as bands 113, 115, 117, and 119, according to their number in the valence band complex of the fully relativistic calculation, counted from below (note that the bands are twofold Kramers degenerate). The AFM-LSDA calculations of the group No. 99 crystal lattice are also shown in Fig. 3 (bottom). In the AFM structure, all the uranium atoms within one layer are ferromagnetically ordered parallel to the c axis, but there exists antiferromagnetic coupling between adjacent layers. Thus the antiferromagnetic **Q** vector is (0, 0, 1). Both space group No. 99 and No. 129 are simple tetragonal groups, henceforth the same high-symmetry labels are used. As seen from its LDA band structure, PM UPt_2Si_2 exhibits a typically intermetallic behavior without a partial gap at the Fermi energy, unlike URu_2Si_2.[16,17] Rather, in the nonmagnetic state there are several nearly flat bands close to E_F, for example bands 115 and 117 along the A-R-Z direction. Specifically, a van Hove singularity can be observed in band 117 along the A-R high-symmetry line. These flat bands will create a high density of states (DOS) at E_F which is, however, unfavorable for the system; through an electronic ordering such as antiferromagnetism, the high DOS peak can effectively be reduced (see the discussion below). The influence of the magnetic exchange splitting is most pronounced along the Γ-M-X and A-R-Z high-symmetry lines (see Fig. 3). Along Γ-M in the nonmagnetic phase, there are degenerate crossing points of the bands 113 and 115, one just below and one just above E_F. AFM ordering induces a lifting of the degeneracy, and, as a consequence, the two bands become fully separated. Similarly, along A-R-Z there are in the nonmagnetic phase degenerate crossings of bands 117 and 119 at the Fermi energy. Again, AFM exchange splitting leads to a removal of these degenerate states and induces the opening of a small partial gap in the AFM phase. Johannsen *et al.*[19] found the emergence

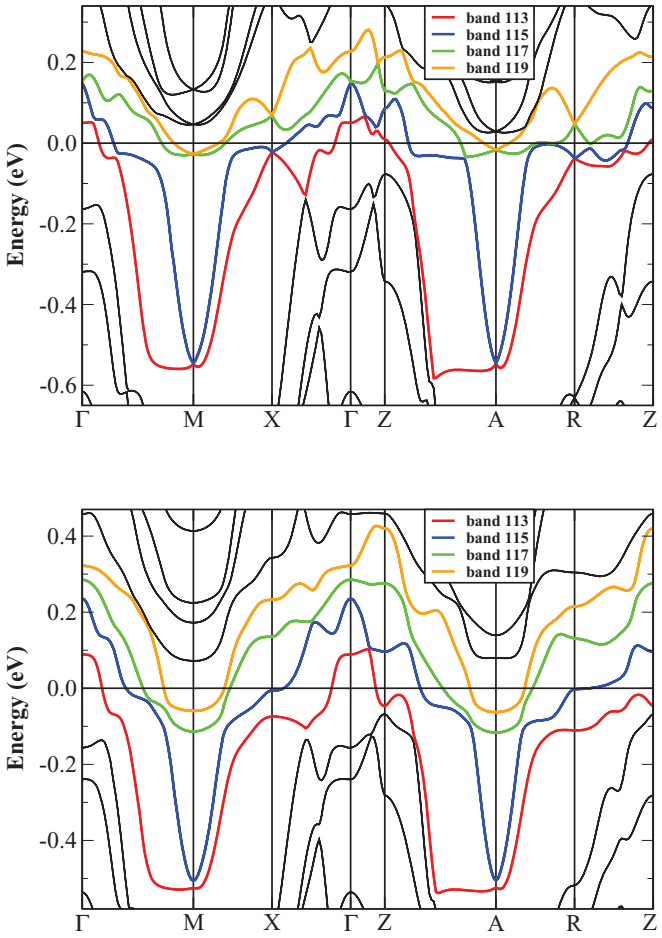

FIG. 3. (Color online) Calculated L(S)DA energy dispersions of the nonmagnetic (top) and antiferromagnetic (bottom) phases of UPt_2Si_2 for space groups No. 129 (PM) and No. 99 (AFM), respectively, for the experimental lattice parameters.

of a large Nernst signal in UPt_2Si_2 below T_N accompanied by anomalies in the thermopower and the Hall coefficient which might be due to the formation of Fermi surface gapping or reconstruction, while the resistivity measurements show no sign of a metal-to-insulator transition but the temperature derivative $d\rho/dT$ changes abruptly at T_N. These observations are consistent with the band-structure calculations, which predict a partial gapping evolving upon AFM ordering, and not a metal-to-insulator transition.

An investigation of the orbital character of the bands near the Fermi level is shown in Fig. 4. The thicknesses of the LSDA bands in the AFM phase show that the bands crossing E_F are dominated by uranium $5f_{5/2}$ states [gray (red)] being hybridized mainly with the Pt $5d$ states [light gray (green)]. These together create a metallic bond while the uranium $5f_{7/2}$ states [dark gray (blue)] are mostly unoccupied. The Pt $5d$ states are weakly present in the whole range of the valence band energies. Hence, the DOS around the Fermi level is dominated by the uranium $5f_{5/2}$ states.

The band structures of antiferromagnetic UPt_2Si_2 have also been determined using the orbital polarization correction as well as the LSDA + U method. For the LSDA + OPC calculation, we do not show the computed bands separately, as

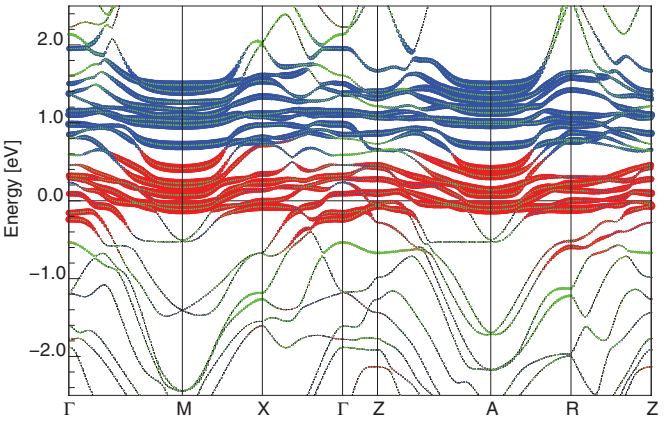

FIG. 4. (Color online) Band character present in the LSDA energy bands calculated for the AFM phase of UPt_2Si_2. The amount of $5f$ character in each of the bands is indicated by the thickness of the band [amount of $5f_{5/2}$ character by gray (red), amount of $5f_{7/2}$ by dark gray (blue), amount of Pt $5d$ character by light gray (green)].

the changes in the band structure are not large. However, we mention that in the vicinity of the M and A high-symmetry points, one more band "dips" below E_F, leading to one more FS sheet in this k-space region (this will be clear from the FS figures given below).

The Hubbard-U correction leads to a more pronounced modification of the band structure. In particular, the LSDA + U calculation (with $U = 2$ eV, $J = 0.5$ eV) redistributes the U $5f$ states around the Fermi level; see Fig. 5. The occupied $5f$ states are moved down in energy, forming now relatively flat bands at around 0.5–1.0 eV under E_F. The unoccupied states cover a bit wider energy range centered around 1.5 eV above E_F where relatively flat bands are formed. These are well visible as peaks in the density of states (see below). On the other hand, in the closest vicinity of the Fermi level, the presence of uranium states is reduced by including the on-site Coulomb U correlation.

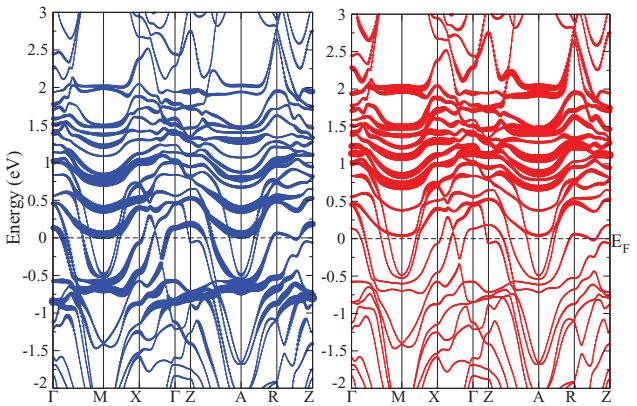

FIG. 5. (Color online) Band structure of AFM UPt_2Si_2 calculated by the LSDA + U method, for $U = 2$ eV and $J = 0.5$ eV. The thickness of the bands corresponds to the amount of spin-up character (left) or spin-down character (right) of a selected uranium atom in the band.

C. Density of states

Figure 6 displays the DOS for the phases PM and AFM, calculated with the L(S)DA, and AFM computed with the orbital polarization correction, respectively. There is a very large U $5f$ DOS peak at E_F in the nonmagnetic calculation, while for the AFM phase a splitting of this peak is realized, causing a significant reduction of the DOS at E_F in the AFM phase. By applying the OPC, a large portion of the U $5f$ DOS is shifted to farther above E_F. The measured linear-temperature specific-heat coefficient of UPt_2Si_2 is about 32 mJ/mol K^2, implying that UPt_2Si_2 is not a strongly correlated or heavy-fermion material.[3] The unrenormalized electronic specific-heat coefficient can be estimated from the

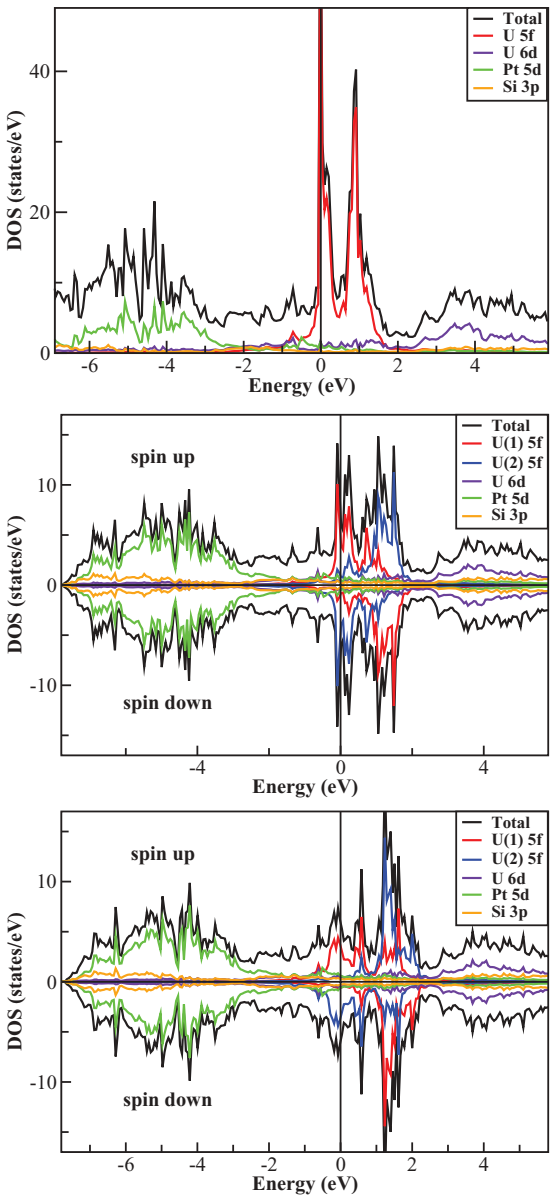

FIG. 6. (Color online) Calculated total and partial DOS of UPt_2Si_2 (for two formula units). Shown are the DOS for the PM phase (top panel) and AFM phase (middle panel), computed with the LSDA, and for the AFM phase computed with LSDA + OPC (bottom panel), using the experimental lattice constants.

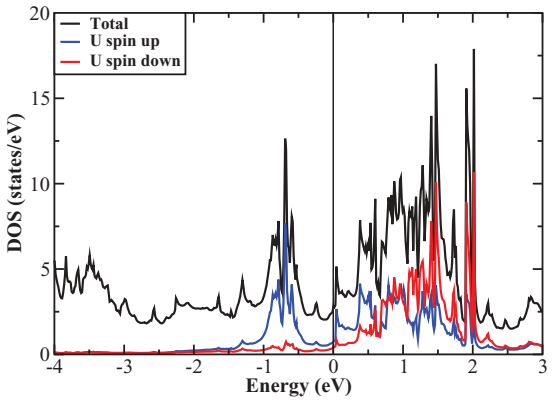

FIG. 7. (Color online) Density of states of AFM UPt_2Si_2 calculated with the LSDA + U method. The total DOS is shown by the black curve, and the dark gray (blue) and gray (red) curves depict spin-resolved DOS of one uranium atom.

DOS calculations by using $\gamma = \frac{1}{3}\pi^2 k_B^2 N(E_F)$, where k_B is the Boltzmann constant and $N(E_F)$ is the density of states at the Fermi energy as determined from the band-structure calculation. The unrenormalized specific-heat coefficients calculated with the L(S)DA for the nonmagnetic and AFM phases are 27 and 18 mJ/mol K^2, respectively, i.e., smaller than the experimental value. LSDA + OPC and LSDA + U give smaller values of 14 and 7 mJ/mol K^2, respectively, for the AFM phase.

In Fig. 7 , we show the DOS obtained from the LSDA + U calculation. The DOS follows the description of the band structure shown in Fig. 5. The partial DOS corresponding to one of the AFM U atoms is substantially reduced at the Fermi level due to the on-site Coulomb correlations, which push the occupied and unoccupied states away from each other on the energy axis. The peak of occupied states is between 0.5 and 1.0 eV under the Fermi level, quite different from that of the LSDA + OPC calculation. The unoccupied states form two sharp peaks around 1.5 and 2.0 eV above E_F. The distribution of the unoccupied states also differs from that calculated by LSDA + OPC. An interesting feature is a small peak in DOS that forms right above the Fermi level.

D. Magnetic properties

As mentioned above, the ground state of UPt_2Si_2 was computed to be the antiferromagnetically ordered phase. The total energy of the latter phase is deeper than the nonmagnetic phase by 56 meV per f.u. Experimentally, the ground state was found to be antiferromagnetic with a total U moment of $1.7\mu_B$ at 4.2 K (Ref. 3) or $2.5\mu_B$ (Ref. 7) along the c axis measured by neutron diffraction. In Table I, we give the computed spin (μ_S), orbital (μ_L), and total moment (μ_J) obtained with the LSDA, LSDA + OPC, and LSDA + U for AFM UPt_2Si_2. The LSDA calculations provide a reasonably large value for the spin moment ($-1.60\mu_B$), but the total moment ($0.71\mu_B$) becomes too small in comparison to the experiments (1.7 to $2.5\mu_B$; see Refs. 3 and 7). This could be due to a weakness of the LSDA calculations, i.e., an absence of optimization of the orbital polarization, tending to give a too small value of the orbital moment.[27] The LSDA + OPC approach was developed

TABLE I. Calculated values of the ordered spin (μ_S), orbital (μ_L), and total (μ_J) magnetic moments (in μ_B) for the AFM arrangement of moments along the c axis. Experimental values[3,7] for the total moment are also given.

Moment	LSDA	LSDA + OPC	LSDA + U	Expt.
μ_S	−1.60	−1.89	−1.76	
μ_L	2.31	3.95	0.39	
μ_J	0.71	2.06	− 1.37	1.7–2.5

to remedy this shortcoming. For UPt_2Si_2, it substantially increases the orbital moment, which now becomes almost $4\mu_B$, whereas the spin moment is only slightly increased. As a result, the total moment of $2.06\mu_B$ is consistent with the experimental values spanning 1.7 to $2.5\mu_B$. The spin moment obtained with the LSDA + U approach is similar to those obtained with LSDA and LSDA + OPC, but the orbital moment is much reduced ($0.39\mu_B$), and is in addition much smaller than the spin moment, which is unusual for uranium compounds. Also, the total moment has become too small compared to the experimental values. Consequently, the LSDA + U approach does not give a satisfactory description of UPt_2Si_2. As the LSDA + U approach is expected to provide an appropriate description for moderately localized f or d electrons, we infer that the $5f$ electrons in low-temperature UPt_2Si_2 are not localized.

E. Fermi surfaces

We have evaluated the Fermi surface (FS) of UPt_2Si_2 applying the LDA, LSDA, LSDA + OPC, and LSDA + U approaches (see Fig. 8). The LSDA FS of nonmagnetic UPt_2Si_2, shown in the top panels of Fig. 8, consists of four sheets, due to the aforementioned four bands crossing E_F. Apart from the relatively small closed FS around the Γ point, the FS sheets have a rather two-dimensional character. The FSs of AFM UPt_2Si_2 are also computed to have a two-dimensional character. The LSDA predicts pronounced changes in the FS sheet of band 115 (second from left panel in Fig. 8). The topology of this sheet clearly changes upon AFM ordering from being partially semispherical to being much more open and two-dimensional. The FS in the LSDA + OPC phase has five sheets, as one new sheet appears along the M-A axis. The LSDA + U calculation predicts again four doubly degenerate bands crossing the Fermi level (see Fig. 5). The topology of this Fermi surface resembles most closely that of LSDA + OPC, although there do exist some minor differences in the two lowest bands. These bands are the least two-dimensional, and generally their exact topology depends more sensitively on the chosen calculation method. As mentioned before, there

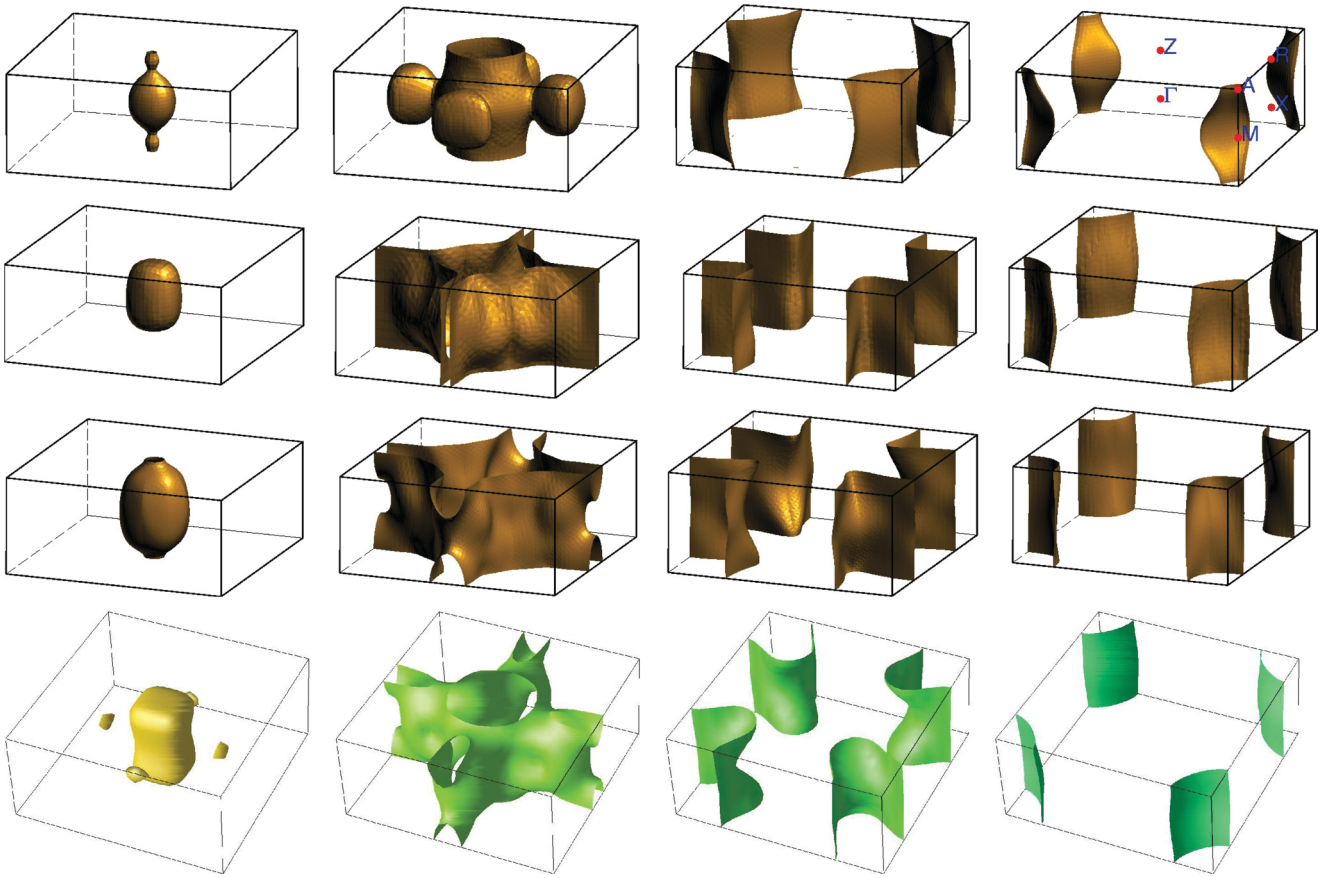

FIG. 8. (Color online) Calculated Fermi surfaces of UPt_2Si_2. Shown are the Fermi surface sheets for the nonmagnetic (top row) and antiferromagnetic phases, calculated with the L(S)DA (second row), and those of the AFM phase obtained with LSDA + OPC (third row) and with LSDA + U (bottom row). The Fermi surface sheets correspond, from left to right, to the bands 113, 115, 117, 119, and 121.

are degenerate band crossings as well as flat band parts at the Fermi energy in the PM phase (Fig. 3, top), which are modified in the AFM phase. Applying only a small shift to the Fermi energy, we found that the topology (orbital contours and gapping regions) of these FSs markedly changed (not shown). Also, within the AFM phase the $z \rightarrow -z$ mirror symmetry of the FSs can be seen to be broken.

In all the phases, the Fermi surface sheets for all bands (except 113) have a rather two-dimensional character, which is consistent with the observed two-dimensional character of the resistivity.[7] The dominant changes in the FS upon AFM ordering occur in the second FS sheet.

In the Fermi surface of URu_2Si_2, a pronounced FS nesting with nesting vector $\mathbf{Q} = (0, 0, 1)$ was recently identified.[17,34] We cannot identify a similar pronounced nesting from the FSs of UPt_2Si_2. For URu_2Si_2, the Fermi energy is computed to fall in a pseudogap in the PM phase, yet the strong nesting is favorable for a folding of the BZ giving a further reduction of the DOS at E_F.[17] In contrast, there is a very high DOS at the Fermi energy in UPt_2Si_2, which can become reduced by the symmetry-breaking AFM transition, without being aided by an antiferromagnetic nesting vector.

IV. SUMMARY AND CONCLUSIONS

We have studied by means of *ab initio* relativistic, spin-polarized band-structure methods the electronic structure of the antiferromagnetic compound UPt_2Si_2, and we compared our results to the experimental features. From the minimum in the total energy calculation, we found that UPt_2Si_2 forms in the less symmetric $P4/nmm$ structure rather than $I4/mmm$, as occurs for URu_2Si_2. Note that Pt is a larger ion possessing two additional d electrons when compared to Ru. The $P4/nmm$ structure for UPt_2Si_2 is stable, i.e., no new crystallographic phases are predicted or found as a function of pressure up to 25 GPa.[33] However, the structure is susceptible to disorder.[7,8] The calculated total energy versus volume for the three possible magnetic phases—PM, FM, and AFM—shows very good agreement with the theoretical equilibrium volume, and a lower minimum is obtained for the antiferromagnetic ground state. The energy dispersions have been calculated for the PM (group No. 129) and AFM (No. 99) phases. PM UPt_2Si_2 computed with the LDA shows typical intermetallic behavior with a large DOS at E_F but without signs of a pseudogap at E_F; rather, in contrast to URu_2Si_2, nonmagnetic UPt_2Si_2 exhibits a very high DOS peak at E_F. As expected, upon AFM ordering, the exchange splitting gives a favorable lifting of PM band degeneracies, which causes a small partial FS gapping, thereby lowering the DOS at E_F. Such partial AFM-FS gapping was suggested in the Nernst experiment of Ref. 19. The bands crossing E_F are dominated by U $5f_{5/2}$ states, which are hybridized with the Pt $5d$ states to enhance the PM DOS.

By comparing the various methods (LSDA, LSDA + OPC, and LSDA + U) of calculating the electronic structure, DOS, and magnetic moment with experiment, the more favorable agreement is obtained with that of LSDA or LSDA + OPC (see Table I). This indicates that UPt_2Si_2 can be better described as an itinerant system rather than a localized U material. A similar conclusion was recently reached in Ref. 15 according to high magnetic field experiments.

The different FS sheets computed with the LSDA, LSDA + OPC, and LSDA + U functionals show a pronounced two-dimensional character for all bands except for the closed surface band 113. As shown in Fig. 8, the FS structure is distinctly different between the PM and AFM phases. Yet among the various calculational methods, similar 2D-shaped FSs result that may be related to the anisotropy in the resistivity and magnetic moment alignment. Unfortunately measurements of the FS, such as ARPES and quantum oscillations, are not available for a direct comparison. We conclude with the following description of UPt_2Si_2 based on our DFT electronic calculations and comparisons with experiment. The material is an itinerant antiferromagnet with moderate magnetic moments resulting from a large orbital moment. In the PM state, the moderate specific-heat coefficient is due to the significant DOS at E_F, which is then reduced as AFM order occurs. Its crystal structure ($P4/nmm$) is stable, and because of its lower symmetry it supports structural disorder. The calculated 2D character is seen in the measured magnetic and scattering anisotropy. Accordingly, further FS measurements are called for to complete and further test the predictions obtained from the electronic structure calculations.

ACKNOWLEDGMENTS

We acknowledge helpful discussions with S. Süllow. This work was supported by the Swedish Reseach Council (VR), Faculty of Science of the University of Johannesburg and the Swedish National Infrastructure for Computing (SNIC).

*On leave from Department of Physics, Menoufia University, Shebin El-kom, Egypt.

[1] K. Hiebl and P. Rogl, J. Nucl. Mater. **144**, 193 (1987).
[2] T. T. M. Palstra, A. A. Menovsky, G. J. Nieuwenhuys, and J. A. Mydosh, J. Magn. Magn. Mater. **54–57**, 435 (1986).
[3] R. A. Steeman, E. Frikkee, S. A. M. Mentink, A. A. Menovsky, G. J. Nieuwenhuys, and J. A. Mydosh, J. Phys.: Condens. Matter **2**, 4059 (1990).
[4] T. Endstra, G. J. Nieuwenhuys, and J. A. Mydosh, Phys. Rev. B **48**, 9595 (1993).
[5] J. A. Mydosh and P. M. Oppeneer, Rev. Mod. Phys. **83**, 1301 (2011).
[6] Y. Kasahara, T. Iwasawa, H. Shishido, T. Shibauchi, K. Behnia, Y. Haga, T. D. Matsuda, Y. Ōnuki, M. Sigrist, and Y. Matsuda, Phys. Rev. Lett. **99**, 116402 (2007).
[7] S. Süllow, A. Otop, A. Loose, J. Klenke, O. Prokhnenko, R. Feyerherm, R. W. A. Hendrikx, J. A. Mydosh, and H. Amitsuka, J. Phys. Soc. Jpn. **77**, 024708 (2008).
[8] M. Bleckmann, A. Otop, S. Süllow, R. Feyerherm, J. Klenke, A. Loose, R. W. A. Hendrikx, J. A. Mydosh, and H. Amitsuka, J. Magn. Magn. Mater. **322**, 2447 (2010).

[9]Z. Henkie, A. Pietraszko, A. Wojakowski, L. Kepinski, and T. Cichorek, J. Alloys Compds. **317-318**, 52 (2001).
[10]T. Cichorek, Z. Henkie, P. Gegenwart, M. Lang, A. Wojakowski, M. Dischner, and F. Steglich, J. Magn. Magn. Mater. **226–230**, 189 (2001).
[11]A. Otop, S. Süllow, M. B. Maple, A. Weber, E. W. Scheidt, T. J. Gortenmulder, and J. A. Mydosh, Phys. Rev. B **72**, 024457 (2005).
[12]Y. B. Ning, J. D. Garrett, C. V. Stager, and W. R. Datars, Phys. Rev. B **46**, 8201 (1992).
[13]S. Süllow, I. Maksimov, A. Otop, F. J. Litterst, A. Perucchi, L. Degiorgi, and J. A. Mydosh, Phys. Rev. Lett. **93**, 266602 (2004).
[14]D. Schulze Grachtrup, M. Bleckmann, S. Süllow, B. Willenberg, H. Rakoto, Y. Skourski, and J. A. Mydosh, J. Low Temp. Phys. **159**, 147 (2010).
[15]D. Schulze Grachtrup, M. Bleckmann, B. Willenberg, S. Süllow, M. Bartkowiak, Y. Skourski, H. Rakoto, I. Sheikin, and J. A. Mydosh, Phys. Rev. B **85**, 054410 (2012).
[16]S. Elgazzar, J. Rusz, M. Amft, P. M. Oppeneer, and J. A. Mydosh, Nat. Mater. **8**, 337 (2009).
[17]P. M. Oppeneer, J. Rusz, S. Elgazzar, M.-T. Suzuki, T. Durakiewicz, and J. A. Mydosh, Phys. Rev. B **82**, 205103 (2010).
[18]I. Kawasaki, S.-i. Fujimori, Y. Takeda, T. Okane, A. Yasui, Y. Saitoh, H. Yamagami, Y. Haga, E. Yamamoto, and Y. Ōnuki, Phys. Rev. B **83**, 235121 (2011).
[19]N. Johannsen, S. Süllow, A. V. Sologubenko, T. Lorenz, and J. A. Mydosh, Phys. Rev. B **78**, 121103 (2008).
[20]S. S. Abelskii and Y. P. Irkhin, Sov. Phys. Solid State **13**, 2035 (1972).
[21]E. G. Dik and S. S. Abelskii, Sov. Phys. Solid State **17**, 454 (1975).
[22]K. Koepernik and H. Eschrig, Phys. Rev. B **59**, 1743 (1999).
[23]P. Blaha, K. Schwarz, G. K. H. Madsen, D. Kvasnicka, and J. Luitz, *WIEN2k, An Augmented Plane Wave + Local Orbitals Program for Calculating Crystal Properties* (Karlheinz Schwarz, Techn. Universtät Wien, Vienna, 2001).
[24]I. Opahle, Ph.D. thesis, University of Technology Dresden, 2001.
[25]H. Eschrig, M. Richter, and I. Opahle, in *Relativistic Electronic Structure Theory Part II: Applications*, edited by P. Schwerdtfeger (Elsevier, Amsterdam, 2004), pp. 723–776.
[26]J. P. Perdew and Y. Wang, Phys. Rev. B **45**, 13244 (1992).
[27]M. S. S. Brooks, Physica B **130**, 6 (1985).
[28]H. Eschrig, M. Sargolzaei, K. Koepernik, and M. Richter, Europhys. Lett. **72**, 611 (2005).
[29]J. Kuneš, P. Novák, M. Diviš, and P. M. Oppeneer, Phys. Rev. B **63**, 205111 (2001).
[30]M. T. Czyzyk and G. A. Sawatzky, Phys. Rev. B **49**, 14211 (1994).
[31]Brillouin zones are from the Bilbao crystallographic server, http://www.cryst.ehu.es.
[32]F. D. Murnaghan, Am. J. Math. **59**, 235 (1937).
[33]K. Sengupta and M. Abd-Elmeguid (private communication). See also S. Ikeda *et al.*, J. Phys. Soc. Jpn. **75**, 125003 (2006).
[34]P. M. Oppeneer, S. Elgazzar, J. Rusz, Q. Feng, T. Durakiewicz, and J. A. Mydosh, Phys. Rev. B **84**, 241102(R) (2011).